# Low-Pass NGD Digital Circuit Application for Real-Time Greenhouse Temperature Prediction

Blaise Ravelo, Mathieu Guerin, Lala Rajaoarisoa, Wenceslas Rahajandraibe

# Low-Pass NGD Digital Circuit Application for Real-Time Greenhouse Temperature Prediction

Blaise Ravelo, *Member*, *IEEE*, Mathieu Guerin, *Member*, *IEEE*, Lala Rajaoarisoa, *Member*, *IEEE*, and Wenceslas Rahajandraibe, *Member*, *IEEE*

***Abstract*—An original application of low-pass (LP) negative group delay (NGD) digital circuit for real-time prediction of greenhouse temperature is investigated. Synthesis formulas allowing to determine the LP-NGD parameters in function of the targeted time-advance are established. The characterization technique of LP-NGD digital circuit implemented on microcontroller platform is validated with a deterministic analytical and real temperature slow pulse signals presenting several hour time-duration. The real-time temperature prediction is tested by employing a commercial temperature sensor in the greenhouse environment. As expected, very good prediction of greenhouse temperature is observed. The experimental result demonstrates an outstanding prediction of ambient temperature variation with -30 minutes time-advance during more than fifty-hour or more than two-day real-time sensing. The present research result opens an innovative roadmap for the future smart buildings and industries where the temperature control and monitoring are particularly key challenging tasks.**

***Index Terms*— Negative group delay (NGD), Real-time predictor, Low-pass (LP) NGD digital circuit, Time-advance, Slow signal processing, Ambient temperature sensing.**

## I. Introduction

DESPITE the spectacular technology progress, the time-delay effect limits considerably communication system performance [1]. To cancel out such an effect, unconventional technique using the counterintuitive negative group delay (NGD) electronic circuit was introduced [2]. But so far, the NGD engineering is still not familiar to most of industrial engineers. Further NGD academic research work is needed for non-specialist engineers. So far, NGD theory investigation, design method, and experimentation were developed in the literature notably with analog electronic circuits [3-16]. The most fascinating NGD effect particularly difficult to understand is its ability to propagate pulse signals in time-advance [3-7]. It should be emphasized that this NGD signature in the time-domain does not forbid the causality principle [3-4]. For the basic understanding, a fundamental NGD theory inspired from the filter one was initiated in [8]. In difference from the filter analysis which is specified by the transfer function (TF) magnitude, the NGD analysis is based on the group delay (GD) response. The types of low-pass (LP) [9-12] and bandpass (BP) [8,13-14] NGD elementary topologies were identified. The LP-NGD circuits are dedicated to operate with baseband arbitrary waveform signals [9-12]. However, the BP-NGD circuits are expected to operate around specific frequencies and must operate with modulated signals [8,13-14]. Despite this progressive research work, compared to other electronic functions, so far, the NGD electronic circuits were not explored enough. Few applications such as delay compensation [2] and medical signal prediction [15-16] were proposed. But most of existing NGD prediction applications are still limited to time-advance less than second or millisecond or microsecond time scales because of analog circuit limitation [9-12]. Such time scale limitations do not allow NGD circuits to operate significantly with slow signals as the environment temperature variations. This application case is a crucial challenge for the societal and industrial development notably for Internet of Things (IoT) and smart building [17-19]. Different building thermal models enable the classification of slow signal types representing the temperature variation information [17-19]. But the main challenge today is the development of relevant prediction control techniques taking into account the climate and weather environment effect [23-24]. One of the most promising solutions to perform the prediction with a large time scale range even up to several minutes can be a crucial application of NGD digital circuits [25-26]. Compared to the NGD analog ones [9-12], very few research works were performed on the digital circuit theory and design. Today NGD research direction must focus on the application development. For this reason, in this paper, an original research work on LP-NGD digital circuit application is explored.

This manuscript received xxx xx 2023; revised xxx xx, 2023; accepted xxx xx, 2023. Date of publication xxx xx, 2023. (Corresponding author e-mail: mathieu.guerin@im2np.fr)

Blaise Ravelo is with the Nanjing University of Information Science & Technology, Nanjing, China (e-mail: blaise.ravelo@yahoo.fr)

Mathieu Guerin and Wenceslas Rahajandraibe are with the Aix-Marseille University, CNRS, University of Toulon, IM2NP UMR7334, Marseille, France (e-mail: {mathieu.guerin, wenceslas.rahajandraibe}@im2np.fr)

Lala Rajaoarisoa is with IMT Nord Europe, University of Lille, Centre for Digital Systems, F-59000 Lille, France (e-mail: lala.rajaoarisoa@imt-nord-europe.fr)

## II. Design Formulas of LP-NGD Digital Circuit

This section introduces the description and design formula of the innovative LP-NGD digital predictor.

### A. Description of LP-NGD Circuit Signature

By denoting $s=j2\pi f$ the Laplace variable, the LP-NGD circuit signature is explained by considering $x$-input and $y$-output of TF $C(s)=Y(s)/X(s)$. The associated magnitude and GD are $C(f)=|C(j2\pi f)|$ and $GD(f)=-\partial\{\arg[C(j2\pi f\approx 0)]\}/\partial f\}/(2\pi)$, respectively. So, we have static gain $C(f\approx 0)=1$, NGD value $GD(f\approx 0)=t_n$ and NGD cut-off frequency $GD(f_n)=0$. The

LP-NGD signature can be specified by time-advance $t_n$<0. The sensed real-time temperature $x(t)$ represents the $t$-time dependent arbitrary waveform input signal. The test synoptic of LP-NGD circuit with pulse response $c(t)$ is depicted by Fig. 1(a). The NGD processing can be applied at any instant time $t>|t_n|$. The input and output time-advance are assessed following relationship as $y(t)\approx x(t+t_n)$ as illustrated by Fig. 1(b).

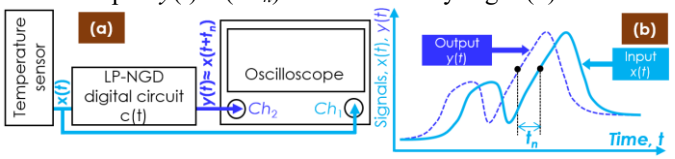


Fig. 1. (a) Synoptic, and LP-NGD predicted (b) input and output signals.

### B. Temperature Sensor and MCU Board Specifications

Fig. 2 represents the test configuration of LP-NGD digital circuit for sensored temperature prediction application. The experimental study is using test protocol proof-of-concept (POC) constituted by commercial: (i) temperature sensor integrated circuit (IC) acting as low-power linear active thermistor referenced MCP9701A-E TO manufactured by Microchip [27], and (ii) the LP-NGD digital circuit implemented on STM32 microcontroller (MCU) board manufactured by STMicroelectronics [28]. The knowledge of sensor technical characteristics is necessary before the LP-NGD digital circuit design which is implemented from active pins. The schematic of interconnection network between sensor and LP-NGD digital circuit is depicted by Fig. 2. The main specifications of the implementation board are microprocessor operating frequency, analog-digital-converter (ADC) and digital-analog converter (DAC) precision as addressed by Table I. During the LP-NGD test, the MCU input analog voltage is limited between $V_{min}$ and $V_{max}$ under quantum resolution $\Delta V$ with sampling period $T_s$.

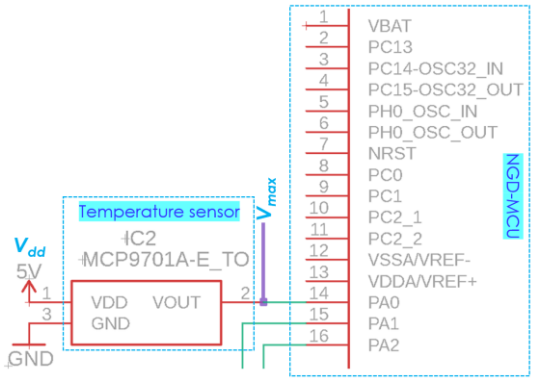


Fig. 2. Temperature sensor and LP-NGD circuit interconnection network schematic.

TABLE I
MCU IMPLEMENTATION BOARD SPECIFICATIONS

| Description | Parameters | Values |
|---|---|---|
| Power supply | $V_{dd}$ | 5 $V_{DC}$ |
| Microprocessor operating frequency | - | 80 MHz |
| Digital resolution | - | 12 bits |
| Quantum resolution | $\Delta V$ | 0.8 mV |
| Input voltage dynamic range | $V_{min}$ (GND) | 0 V |
| | $V_{max}$ | 3.3 $V_{DC}$ |
| Sampling period | $T_s$ | 240 s |

### C. Design Formulas of LP-NGD Digital Predictor

The digital circuit under study is designed from the discretization of LP-NGD canonical form defined in [25-26]. The first order difference equation derived from TF cadenced by sampling period $T_s$ is written as:

$$y[k+1] = c_0x[k] + c_1x[k+1] + c_2y[k] \quad (1)$$

with $k=\{1,2,3,\ldots\}$ and taking $y[1]=x[1]$. By assuming the case of unity static gain TF, the synthesis equations of real coefficients $c_0$, $c_1$ and $c_2$ from the targeted time-advance which represents NGD value $t_n$ and cut-off frequency $f_n$. Therefore, the LP-NGD digital circuit design formulas are expressed:

$$c_0 = [\pi f_n t_n - \sqrt{1+(\pi f_n t_n)^2}]/\xi \quad (2)$$

$$c_1 = [\pi f_n (2T_s - t_n) + \sqrt{1+(\pi f_n t_n)^2}]/\xi \quad (3)$$

$$c_2 = [\pi f_n t_n + \sqrt{1+(\pi f_n t_n)^2}]/\xi \quad (4)$$

with $\xi = \pi f_n (t_n + 2T_s) + \sqrt{1+(\pi f_n t_n)^2}$. It is noteworthy that to get better predicted signal integrity (SI), the sampling and time-advance is desirably respect the condition $t_n \geq 4T_s$. Fig. 3 presents the flow diagram describing the steps of the LP-NGD digital circuit design and implementation.

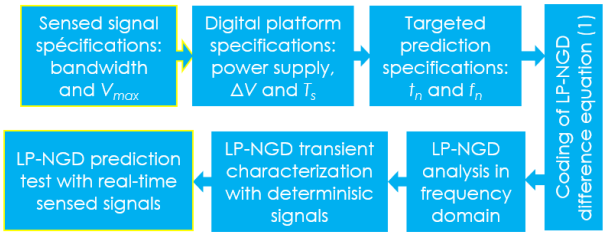


Fig. 3. LP-NGD digital circuit design flow.

Before the real-time temperature prediction validation, it would be necessary to characterize the LP-NGD digital circuit performance with deterministic pulse signal.

## III. CALIBRATION TEST OF REAL-TIME LP-NGD PREDICTOR WITH DETERMINISTIC PULSE SIGNAL

This section introduces the deterministic pulse signal based real-time prediction calibration test of LP-NGD predictor.

### A. Analytical Definition of Deterministic Pulse Test Signal

The test signal should present a pulse waveform in order to assess the input and output time-advance associated to rise and fall edge fronts in addition to the amplitude comparison. In addition, the spectral bandwidth of the pulse test input signal must be lower than $f_n$. In this case, the test signal is an asymmetric Gaussian pulse analytically defined by:

$$x(t) = x_m[e^{-t^2/(2\xi)} - e^{-t^2/\xi}] \quad (5)$$

with amplitude $x_m$=4 and temporal parameter $\xi=A_{db}\log(10)/(5\pi^2 f_n^2)$ by taking $A_{dB}$=20 dB. From the yielded transient result, the time-advance is assessed by equations $x(t)$=1/2 and $y(t+t_n)$=1/2. The amplitude ratio of input and output pulse signal is given by:

$$\alpha = \max[y(t)] / \max[x(t)]. \quad (6)$$

The correlation coefficient (represented by MATLAB function "*corrcoeff*") between the input and output signals is defined by:

$$\gamma_{x,y} = corrcoeff[x(t), y(t)]. \quad (7)$$

The LP-NGD signature is determined by the simulated analog and computed responses of LP-NGD predictor.

### *B. Discussion on LP-NGD Prediction of Deterministic Pulse Slow Signals*

The LP-NGD analog equivalent circuit POC was simulated in the environment of ADS electronic design software commercial tool from Keysight Technologies simulation software. Before the experimentation, the LP-NGD predictor defined by difference equation (1) was implemented into the STM32 MCU test board. The digital MCU implementation platform is a Nucleo L476RG development board. The platform is using an STM32L476RG MCU IC package having 64-pins. The associated digital circuit is coded in C-language program as literally monitored by pseudo-code of Algorithm 1. The LP-NGD predictor coefficients $c_0$=-2.153, $c_1$=2.331 and $c_2$=0.822 are calculated by synthesis formulas (2), (3) and (4). To verify the prediction feasibility with the original LP-NGD predictor, practical tests were performed. Fig. 4(a) represents the comparison between the analog circuit transient responses of asymmetrical Gaussian pulse: (i) input signal $x$ plotted in black solid curve, (ii) output simulated signal $y_{analog}$ from LP-NGD analog circuit simulation plotted in sky-blue solid curve, (iii) output calculated signal $y_{digital}$ from the LP-NGD digital circuit model plotted in red dashed curve and (iv) the experimented output from the implemented LP-NGD digital circuit plotted in navy-blue dashed curve. The calculated, simulated and measured transient results are in good correlation. It can be understood from these results that the transient responses present remarkable signal behavioral prediction. The time-advance can be assessed from zoom in plot within the time interval [0.5 h, 2.5 h] shown in Fig. 4(b).

Algorithm 1. Pseudo-code of implemented LP-NGD predictor.

```
   // c0, c1 and c2: coefficients to be calculated versus targeted time-advance tn
float c0 = -2.153; float c1 = 2.331; float c2 = 0.822;
  // xxx is the initial value of input signal
float x_1 = xxx; float y_1 = x_1;
return float Process(float input)
{  // Update internally stored output at t=k*Ts
   y_0 = y_1;
   // Update internally stored input at t=k*Ts
   x_0 = x_1;
   // Update internally stored input à t=(k+1)*Ts
   x_1 = input;
   // Compute output
   y_1= c0*x_0+ c1*x_1+c2*y_0;
   return y_1; }
```

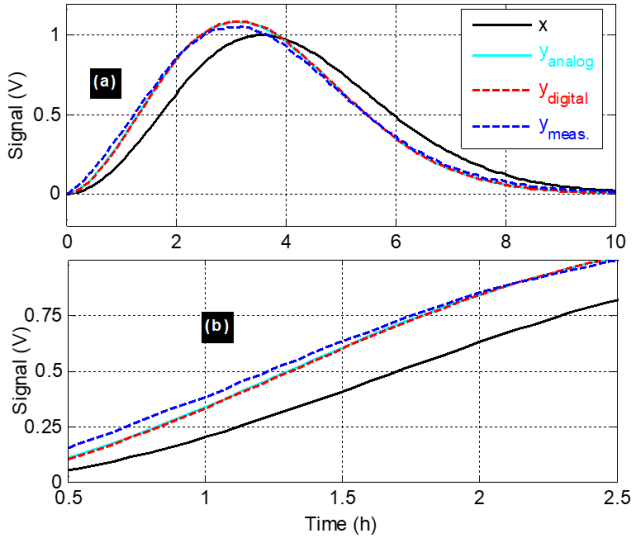


Fig. 4. Transient responses of analog and digital LP-NGD circuits with asymmetric Gaussian: (a) full and (b) [0.5 h, 2.5 h] zoomed in time window.

TABLE II
COMPARISON OF LP-NGD CHARACTERISTICS

| Approach | $\alpha$ | $t_n$ | $\gamma_{x,y}$ |
|---|---|---|---|
| Calculation | 1.09 | -0.442 h | 96% |
| Simulation | 1.09 | -0.441 h | 95.7% |
| Experiment | 1.05 | -0.48 h | 94.8% |

Table II summarizes the obtained time-domain LP-NGD characteristics. Very good correlation coefficients better than 94% confirm the fidelity between input and output SI despite the prediction aspect. After the feasibility study of deterministic signal case prediction, a challenging investigation for more complex test signal was performed by considering ambient temperature as input.

## IV. EXPERIMENTATION OF REAL-TIME LP-NGD PREDICTION APPLIED TO SENSED TEMPERATURE WITH HEATED SENSOR

This section discusses the real-time test of greenhouse temperature sensing with innovative LP-NGD predictor.

### *A. Description of the Greenhouse Based Experimental Setup*

As described by Figs. 5, the LP-NGD predictor experimentation was based on the use of greenhouse exposed to sunny environment of IM2NP (Institut Matériaux Microélectronique Nanosciences de Provence) laboratory in the Marseille city. The test was carried out in typical summer Mediterranean season in south of France. The illustrative synoptic of the carried-out test is displayed by Fig. 5(a). The sensor provides the inside greenhouse temperature denoted $T_{in}$ converted into voltage signal injected into the LP-NGD MCU digital circuit. The test board was fed by $V_{dd}$=5 V via USB connector of driver laptop. The laptop drives the MCU board and also ensures the data processing, acquisition and storage. The experimental setup photograph is depicted by Fig. 5(b). The overall setup is driven by the executed program installed on the laptop. The non-adiabatic greenhouse is a plastic paralleled box having 18 cm×18 cm×15 cm as stressed in Fig. 5(b). After several days of test campaign, the time-domain result was carefully treated. The measured data was saved in the driver and acquisition laptop. The obtained results enabling to compare time-dependent input signal $T_{in}(t)$ and output signal $T_{out}(t)\approx T_{in}(t+t_n)$ is explored in the following subsection.

### *B. Long-Duration Real-Time Test with Greenhouse Environment Temperature LP-NGD Prediction*

The result of the original LP-NGD application test in real-time is analyzed in this paragraph. Thanks to the time-advance effect, one demonstrates that the sensed temperature waveform is very well-predicted by the LP-NGD digital circuit.

To perform the analysis, we denote $T_{in}(t)=x(t)$ the sensed greenhouse ambient temperature. The transient signals generated from the greenhouse ambient temperature shown by the experimental setup displayed in Figs. 5. The real-time recorded output signal of LP-NGD predictor is denoted $T_{out}(t)=y(t)$. Figs. 6 expose the LP-NGD predictor obtained responses. Substantially, a very good correlation between the calculated ("calc." plotted in red solid line plot) and measured ("meas." plotted in dashed blue plot) results from the LP-NGD predictor prototype is confirmed.

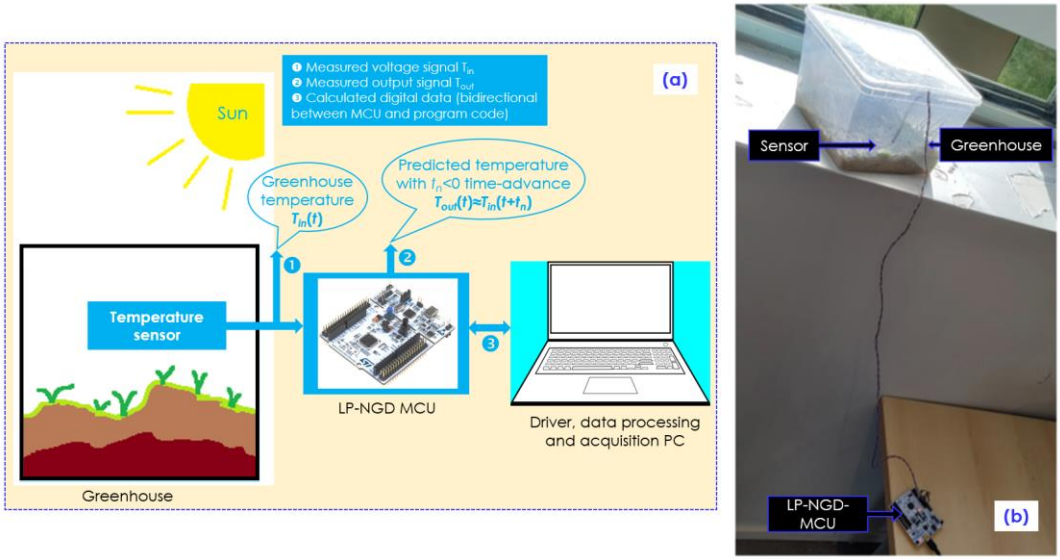


Fig. 5. LP-NGD digital circuit predictor (a) synoptic diagram and (b) photograph of greenhouse temperature sensing scenario.

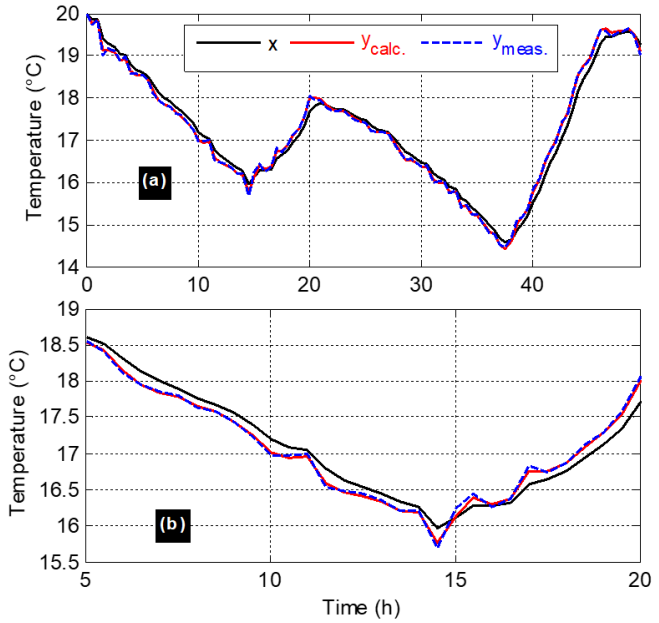


Fig. 6. LP-NGD predicted results from the test protocol shown in Figs. 5 in (a) large and (b) zoomed in window.

We can find that an excellent prediction of greenhouse temperature variation is observed as depicted by Figs. 6. The ambient temperature prediction test was done during $t_{max}$=49.5 h or 2.06 days under sampling period $T_s$=9 s. In this case, by taking $T_{ref}$=17°C, the time-advance was assessed by the following equation system $T_{in}(t)=T_{ref}/2$ and $T_{out}(t+t_n)=T_{ref}/2$. For typical arbitrary waveform signals, the amplitude ratio may not be adequate. However, it can be assessed in different ways depending on the application standard specifications. Despite the signal waveform complexity, the time-advance and input-output signal correlation are assessed like in previous subsection. However, the amplitude ratio between the input and output temperature signals is defined to equation (6). The amplitude ratio is defined from local minimum and maximum of temperature $T_{min}$ and $T_{max}$, in the time range from instant times $t$=12 h to $t$=22 h by:

$$\alpha = \max\left[T_{out,\max}(t) - T_{out,\min}(t)\right] / \max\left[T_{in,\max}(t) - T_{in,\min}(t)\right] . \quad (8)$$

TABLE III
LP-NGD CHARACTERISTIC COMPARISON FROM CALCULATED AND MEASURED RESULTS OF REAL-TIME TEMPERATURE PREDICTOR

| Approach | $\alpha$ | $t_n$ | $\gamma_{x,y}$ |
|---|---|---|---|
| Calculation | 1.12 | -0.49 h | 99.3% |
| Experiment | 1.13 | -0.45 h | 99% |

Even for this long-time duration test, the SI between the LP-NGD predicted and measured temperatures is assessed by the cross correlation $\gamma_{x,y}$. Table III recapitulates the corresponding time-domain LP-NGD characteristics including the input and output signal correlation coefficients. The recapitulated characteristics confirm the time-advance of about 2% and 10% of the targeted one from calculation and experimentation, respectively. The input and output predicted temperature correlation coefficients are better than 99%.

## V. CONCLUSION

A pioneer research work stresses real-time temperature prediction feasibility of ambient environment over some daytime duration. The original predictor is designed by LP-NGD digital circuit. The LP-NGD difference equation parameters are calculated from the targeted time-advance representing the signal prediction. After describing the characterization technique, the innovative predictor is validated by theory, simulation and test.

The LP-NGD predictor POC is synthesized, designed, implemented on MCU board and successfully tested. The digital circuit prototype is implemented on the STM32 MCU platform. The time-domain characterization is based on several hours duration test signal having the asymmetric exponential waveform. A very good agreement between the calculated, simulated and experimented results is pointed out. As expected, the output of LP-NGD digital circuit is observed with -30 min time-advance compared to the corresponding input. One original aspect of the present study is also the demonstration of the half-hour time-advance regarding category of slow signals.

In the future, the proposed sensor signal pre-detection technique can be used to revolutionize the future industrial sensors to perform the industrial facility control.

## REFERENCES


[1] S. Liu, X. Wang and P. X. Liu, "Impact of Communication Delays on Secondary Frequency Control in an Islanded Microgrid," IEEE Tran. Industrial Electronics, vol. 62, no. 4, pp. 2021-2031, Apr. 2015.

[2] D. Solli, R. Y. Chiao, and J. M. Hickmann, "Superluminal effects and negative group delays in electronics, and their applications," Phys. Rev. E, Vol. 66 (056601), pp. 1-12, 2002.

[3] M. W. Mitchell and R.Y. Chiao, "Causality and Negative Group-delays in a Simple Bandpass Amplifier," Am. J. Phys., vol. 66, 1998, pp. 14-19.

[4] M. W. Mitchell and R.Y. Chiao, "Negative Group-delay and 'Fronts' in a Causal Systems: An Experiment with Very Low Frequency Bandpass Amplifiers," Phys. Lett. A, vol. 230, Jun. 1997, pp. 133-138.

[5] T. Nakanishi, K. Sugiyama and M. Kitano, "Demonstration of Negative Group-delays in a Simple Electronic Circuit," Am. J. Phys., vol. 70, no. 11, 2002, pp. 1117-1121.

[6] M. Kitano, T. Nakanishi and K. Sugiyama, "Negative Group-delay and Superluminal Propagation: An Electronic Circuit Approach," IEEE J. Sel. Top. in Quantum Electron., vol. 9, no. 1, Feb. 2003, pp. 43-51.

[7] J. N. Munday and R. H. Henderson, "Superluminal Time Advance of a Complex Audio Signal," Appl. Phys. Lett., vol. 85, July 2004, pp. 503-504.

[8] B. Ravelo, "Similitude between the NGD function and filter gain behaviours," Int. J. Circ. Theor. Appl., vol. 42, no. 10, Oct. 2014, pp. 1016–1032.

[9] B. Ravelo, "First-order low-pass negative group delay passive topology," Electronics Letters, vol. 52, no. 2, Jan. 2016, pp. 124-126.

[10] B. Ravelo, "Methodology of elementary negative group delay active topologies identification," IET Circuits Devices Syst., vol. 7, no. 3, May 2013, pp. 105-113.

[11] M. T. Abuelma'atti and Z. J. Khalifa, "A new CFOA-based negative group delay cascadable circuit," Analog Integrated Circuits and Signal Processing, vol. 95, pp. 351-355, Mar. 2018.

[12] B. Ravelo, W. Rahajandraibe, M. Guerin, B. Agnus, P. Thakur and A. Thakur, "130-nm BiCMOS design of low-pass negative group delay integrated RL-circuit," Int. J. Circ. Theor. Appl., vol. 50, no. 6, Feb. 2022, pp. 1876-1889.

[13] B. Ravelo, "Investigation on microwave negative group delay circuit," Electromagnetics, Vol. 31, No. 8, Nov. 2011, pp. 537-549.

[14] B. Ravelo, "Innovative Theory on Multiband Negative Group Delay Topology Based on Feedback Loop Power Combiner," IEEE Tran. CAS II: Express Briefs, vol. 63, no. 8, Aug. 2016, pp. 738-742.

[15] C. Hymel, R. A. Stubbers, and M. E. Brandt, "Temporally Advanced Signal Detection: A Review of the Technology and Potential Applications," IEEE CAS Magazine, vol. 11, no. 3, pp. 10-25, 2011.

[16] H. U. Voss, "Signal prediction by anticipatory relaxation dynamics," Phys. Rev. E, Vol. 93, No. 3, (030201R), pp. 1-5, 2016.

[17] A. Thavlov and H. W. Bindner, "Thermal Models for Intelligent Heating of Buildings," Proc. of Int. Conference on Applied Energy, ICAE 2012, July 5-8, 2012, Suzhou, China, pp. A10591-A106000.

[18] A. Anjomshoaa, "Blending building information with smart city data," Proc. of the 5th Int. Conf. on Semantics for Smarter Cities, vol. 1280, Oct. 2014, pp. 1-2.

[19] D. I. Vesna Glatz, "Smart buildings & IoT," pdf presentation, EMPOWERING Smart buildings enable productive people, Microsoft, 2016.

[20] S. Goyal, and P. Barooah, "A method for model-reduction of non-linear thermal dynamics of multi-zone buildings," Energy and Buildings, vol. 47, pp. 332-340, 2012.

[21] B. Ravelo, L. Rajaoarisoa and O. Maurice, "Thermal modelling of multilayer walls for building retrofitting," J. Building Engineering, vol. 29, no. 101126, May 2020, pp. 1-11.

[22] R. Randriatsiferana, L. Rajaoarisoa, S. Ngoho, W. Rahajandraibe and B. Ravelo, "Zonal Thermal Room Original Model with Kron's Method," IEEE Access, vol. 8, no. 1, 2020, pp. 174893-174909.

[23] M. H. Benzaama, L. Rajaoarisoa, B. Ajib, S. Lecoeuche, "A data-driven methodology to predict thermal behavior of residential buildings using piecewise linear models," J. Building Eng., vol. 32, 2020, 101523,

[24] L. Rajaoarisoa, B. Ravelo, W. Rahajandraibe and L. Etienne, "Numerical weather modelling to improve energy efficiency and climate control of the buildings," Proc. of Conf. Francophone de l'Int. Building Performance Simulation Association (IBPSA), 12-13 Nov. 2020, Reims, France, pp. 1-5.

[25] B. Ravelo, "Elementary NGD IIR/FIR Systems," Int. J. Signal Processing Systems (IJSPS), vol. 2, no. 2, Dec. 2014, pp. 132-138.

[26] B. Ravelo, M. Guerin, W. Rahajandraibe, V. Gies, L. Rajaoarisoa and S. Lalléchère, "Low-Pass NGD Numerical Function and STM32 MCU Emulation Test," IEEE Trans. Industrial Electronics, vol. 39, no. 8, Aug. 2022, pp. 8346-8355.

[27] Microchip, MCP9700/9700A and MCP9701/9701A, Low-Power Linear Active Thermistor ICs, Datasheet-Production Data, pp. 1-22, June 2022.

[28] ST, STM32L476xx, Datasheet-Production Data, pp. 1-270, June 2019.